10-6-2022

Role of Bifidobacterium pseudocatenulatum in Degradation and Consumption of Xylan-Derived Carbohydrates

Elizabeth Drey

Car Reen Kok

Robert Hutkins

AMERICAN SOCIETY FOR MICROBIOLOGY | Applied and Environmental Microbiology®

PHYSIOLOGY

Role of *Bifidobacterium pseudocatenulatum* in Degradation and Consumption of Xylan-Derived Carbohydrates

Elizabeth Drey,[a,b] Car Reen Kok,[b,c] Robert Hutkins[a,b]

[a]Department of Food Science and Technology, Food Innovation Center, University of Nebraska—Lincoln, Lincoln, Nebraska, USA
[b]Nebraska Food for Health Center, University of Nebraska—Lincoln, Lincoln, Nebraska, USA
[c]Complex Biosystems, University of Nebraska—Lincoln, Lincoln, Nebraska, USA

ABSTRACT Xylans, a family of xylose-based polysaccharides, are dietary fibers resistant to digestion. They therefore reach the large intestine intact; there, they are utilized by members of the gut microbiota. They are initially broken down by primary degraders that utilize extracellular xylanases to cleave xylan into smaller oligomers. The resulting xylooligosaccharides (XOS) can either be further metabolized directly by primary degraders or cross-feed secondary consumers, including *Bifidobacterium*. While several *Bifidobacterium* species have metabolic systems for XOS, most grow poorly on longer-chain XOS and xylan substrates. In this study, we isolated strains of *Bifidobacterium pseudocatenulatum* and observed that some, including *B. pseudocatenulatum* ED02, displayed growth on XOS with a high degree of polymerization (DP) and straight-chain xylan, suggesting a primary degrader phenotype that is rare in *Bifidobacterium*. *In silico* analyses revealed that only the genomes of these xylan-fermenting (xylan$^+$) strains contained an extracellular GH10 endo-β-1.4 xylanase, a key enzyme for primary degradation of xylan. The presence of an extracellular xylanase was confirmed by the appearance of xylan hydrolysis products in cell-free supernatants. Extracellular xylanolytic activity was only detected in xylan$^+$ strains, as indicated by the production of XOS fragments with a DP of 2 to 6, identified by thin-layer chromatography (TLC) and high-performance liquid chromatography (HPLC). Additionally, *in vitro* fecal fermentations revealed that strains with a xylan$^+$ phenotype can persist with xylan supplementation. These results indicate that xylan$^+$ *B. pseudocatenulatum* strains may have a competitive advantage in the complex environment of the gastrointestinal tract, due to their ability to act as primary degraders of xylan through extracellular enzymatic degradation.

IMPORTANCE The beneficial health effects of dietary fiber are now well established. Moreover, low fiber consumption is associated with increased risks of metabolic and systemic diseases. This so-called "fiber gap" also has a profound impact on the composition of the gut microbiome, leading to a disrupted or dysbiotic microbiota. Therefore, understanding the mechanisms by which keystone bacterial species in the gut utilize xylans and other dietary fibers may provide a basis for developing strategies to restore gut microbiome function. The results described here provide biochemical and genetic evidence for primary xylan utilization by human-derived *Bifidobacterium pseudocatenulatum* and show also that cooperative utilization of xylans occurs among other members of this species.

KEYWORDS xylan, xylooligosaccharide, prebiotic, glycoside hydrolase, bifidobacteria, cooperation, xylanase

Xylans are a class of nondigestible polysaccharides that contain a xylose-based backbone with β-1,4 glycosyl linkages. Linear homoxylans are uncommon in foods; rather, most xylans appear in the diet as heteroxylans (1). These heteroxylans are decorated with a variety of other sugars, including arabinose and glucuronic acid in the case of arabinoxylans and

Editor Pablo Ivan Nikel, Novo Nordisk Foundation Center for Biosustainability

Address correspondence to Robert Hutkins, rhutkins1@unl.edu.

The authors declare a conflict of interest. R.H. has received grants and honoraria from several food and ingredient companies, is a co-owner of Synbiotic Health, and was on the Board of Directors of the International Scientific Association for Probiotics and Prebiotics.

[This article was published on 6 October 2022 with an error in reference 12. The reference was corrected in the current version, posted on 26 October 2022.]

Received 2 August 2022
Accepted 16 September 2022
Published 6 October 2022

glucuronoxylans, respectively. Dietary xylan fibers are found predominantly in monocots, including cereal grains, although they can also be found at low levels in the peels of fruits and vegetables (2, 3).

Xylans appear to have evolved as important substrates for fungi and bacteria in a variety of ecological biospheres, including seawater, alkaline hot springs, and the mammalian digestive tract (4–6). These microbes employ enzymatic machinery that includes a combination of xylanases and accessory enzymes that work sequentially to degrade heteroxylan. Xylanases are enzymes that cleave β-1,4 glycosyl linkages between consecutive xylose units in the xylan backbone, while accessory enzymes remove side chains (7). Further xylan degradation requires endoxylanases to cleave the interior regions of the xylan backbone into xylooligomer fractions. These endoxylanases, identified via the carbohydrate-active enzyme (CAZy) database, typically are found in the glycoside hydrolase (GH) families GH5, GH10, GH11, GH30, and GH98 (8, 9).

In humans, xylans are resistant to digestion by digestive enzymes and reach the large intestine intact; there, they are subject to colonic fermentation by members of the gut microbiome (10). These fermenters can be broadly categorized as primary degraders and secondary consumers, based on their ability to degrade xylan and transport and consume xylan hydrolysis products (11, 12). Primary degraders are capable of direct consumption of xylan; most belong to the phyla *Bacteroidetes*, *Actinobacteria*, and *Firmicutes*. For primary degradation of xylan, *Bacteroidetes* express extracellular xylanases that are anchored to the outer membrane and near a SusC/SusD transport system (13). This xylanase degrades xylan into small xylooligosaccharide (XOS) species that are then transported by the SusC/SusD receptor into the periplasm, where further dismantling of the oligosaccharide occurs. Similarly, primary degradation in *Firmicutes* and *Actinobacteria* also relies on an anchored extracellular xylanase, but these Gram-positive bacteria utilize substrate binding proteins and ATP-binding cassettes (ABC) or phosphoenolpyruvate (PEP) phosphotransferase system (PTS) transporters to move XOS substrates directly into the cytoplasm (9).

Other organisms are known to take advantage of the xylooligosaccharide products produced by primary degraders via cross-feeding (14). These secondary consumers include Gram-positive bacteria that lack key extracellular xylanolytic activity for direct degradation of xylan. Two major groups of secondary consumers are *Lactobacillaceae* and *Bifidobacterium*, which utilize highly specialized substrate recognition and transport systems for detection and transport of XOS (9). *In vitro* and *in vivo* studies suggest that XOS is more effective at stimulating growth of *Bifidobacterium* species than *Lactobacillaceae*, and XOS is also considered more selective than other prebiotic oligosaccharides (15–17). Even within *Bifidobacterium*, XOS utilization is highly specific, with many XOS-metabolizing strains able to grow only on XOS with a low degree of polymerization (DP) (18). Therefore, growth on high-DP XOS and xylan fragments appears to be a rare trait in *Bifidobacterium*.

Among *Bifidobacterium* species having such a phenotype are strains of *Bifidobacterium pseudocatenulatum*. This species is generally considered an adult-type *Bifidobacterium*, although strains have also been isolated from breastfed infants and children (19–21). This species is clustered in the *Bifidobacterium adolescentis* phylogenetic group and has been shown to ferment a diverse array of carbohydrate sources potentially present in the adult diet (12, 22). Some strains have also been reported to have probiotic or health-promoting properties (23–25).

We previously identified strains of *B. pseudocatenulatum* that were enriched *in vitro* during growth on XOS (26). Preliminary experiments revealed that several of these strains also grew well on longer-chain XOSs and xylan, indicating a potentially novel phenotype in *Bifidobacterium*. Recently, very similar phenotypes were also described for strains of this species (12). In this study, we extended these findings by comparing the abilities of five *B. pseudocatenulatum* strains to grow on xylan and low-DP and high-DP XOSs. Growth on these xylose-based substrates was dependent on the presence of relevant enzymes and corresponding gene clusters in their genomes. However,

TABLE 1 Growth of five sequenced *Bifidobacterium pseudocatenulatum* strains on various xylose-based carbohydrates

	Growth of indicated strain[a]				
Substrate	**ED01**	**ED02**	**ED03**	**CR16**	**ED05**
Glucose	+++	+++	+++	+++	+++
Xylose	−	++	−	−	−
Xylan	−	++	++	−	−
Short XOS (enriched in DPs of ≤4)	++	+++	+++	++	++
Long XOS (enriched in DPs of >4)	+	+++	+++	+	+
Arabinoxylan	−	−	−	−	−
Basal	−	−	−	−	−

[a]Growth phenotypes were based on optical density at 600 nm after 24 h of incubation in basal MRS containing 0.5% of the indicated carbohydrates. −, growth at OD of <0.1; +, growth at 0.1> OD < 0.2; ++, growth at 0.2> OD < 0.45; +++, growth at OD of >0.45.

we also observed that strains that were unable to consume large-DP XOSs directly could still grow on these substrates. This findings suggest that cross-feeding reactions may provide a basis for cooperative utilization of these substrates within this species.

RESULTS

Growth characteristics of *Bifidobacterium* strains and isolates. We evaluated the abilities of five *B. pseudocatenulatum* strains (ED01, ED02, ED04, ED05, and CR16), previously isolated from XOS enrichment experiments (see Materials and Methods), to grow in modified deMan, Rogosa, and Sharpe (mMRS) broth containing xylan and XOS (Table 1). Glucose was used as the positive control, while medium without added carbohydrates was used as the negative control. All strains were able to grow on 0.5% XOS (XOS$^+$), with strains ED02 and ED03 displaying growth comparable to that on glucose (optical density at 600 nm [OD_{600}] after 24 h > 0.45) on both short XOSs (SXOSs; enriched in members with a DP of ≤4) and long XOSs (LXOSs; enriched in members with a DP of >4). In contrast, strains ED01, CR16, and ED05 had moderate growth (arbitrarily assigned when the 0.2 < OD < 0.45) on SXOS and weak growth (0.1 > OD < 0.2) on LXOS. In addition, strains ED02 and ED03 were also able to grow on xylan (OD_{600} > 0.30) (xylan$^+$), whereas strains ED01, CR16, and ED05 demonstrated no growth (xylan$^-$). Additionally, none of the strains grew on arabinoxylan or in the negative controls. For subsequent experiments, ED01 and ED02 were selected as representative xylan$^-$ and xylan$^+$ strains, respectively (Fig. 1A).

In addition to the five selected strains, 10 additional *B. pseudocatenulatum* strains isolated from different subjects and 9 strains of other *Bifidobacterium* species were screened for growth on xylan, LXOSs, and xylose. Overall, the *B. pseudocatenulatum* strains could be arranged into four phenotypes based on their growth on all three xylan substrates (see Table S1 in the supplemental material). Interestingly, ED03 was the only strain that had a xylan$^+$ and XOS$^+$ phenotype but did not grow on xylose. Furthermore, in some instances, isolates obtained from the same subjects displayed different growth phenotypes. Based on growth on xylan, LXOS, and xylose, the other *Bifidobacterium* species were grouped into one of three additional phenotypes (Table S1). However, none of these strains grew on xylan, and only three grew well on LXOS.

Genomic evidence for the presence of GH10 xylanases in *Bifidobacterium*. *In silico* analysis of carbohydrate-active gene clusters (CGCs) in the sequenced *B. pseudocatenulatum* genomes revealed the presence of three major clusters associated with XOS utilization (Fig. 1B; Fig. S1). These three clusters contain substrate binding proteins, transporters, and key glycosyl hydrolases that were shown to act on xylose-based substrates, as described in the CAZy database. First, we observed that the genomes of all five strains contained all genes within XOS-active cluster III. This cluster includes genes for a substrate binding protein, two ABC transporter permeases, a transcriptional regulator, and two GH43 glycosyl hydrolases. However, cluster I and cluster II were not entirely conserved between the xylan$^+$ and xylan$^-$ strains. Compared to the case with xylan$^+$ strains ED02 and ED03, XOS active cluster I in strains ED01 and CR16 lacked

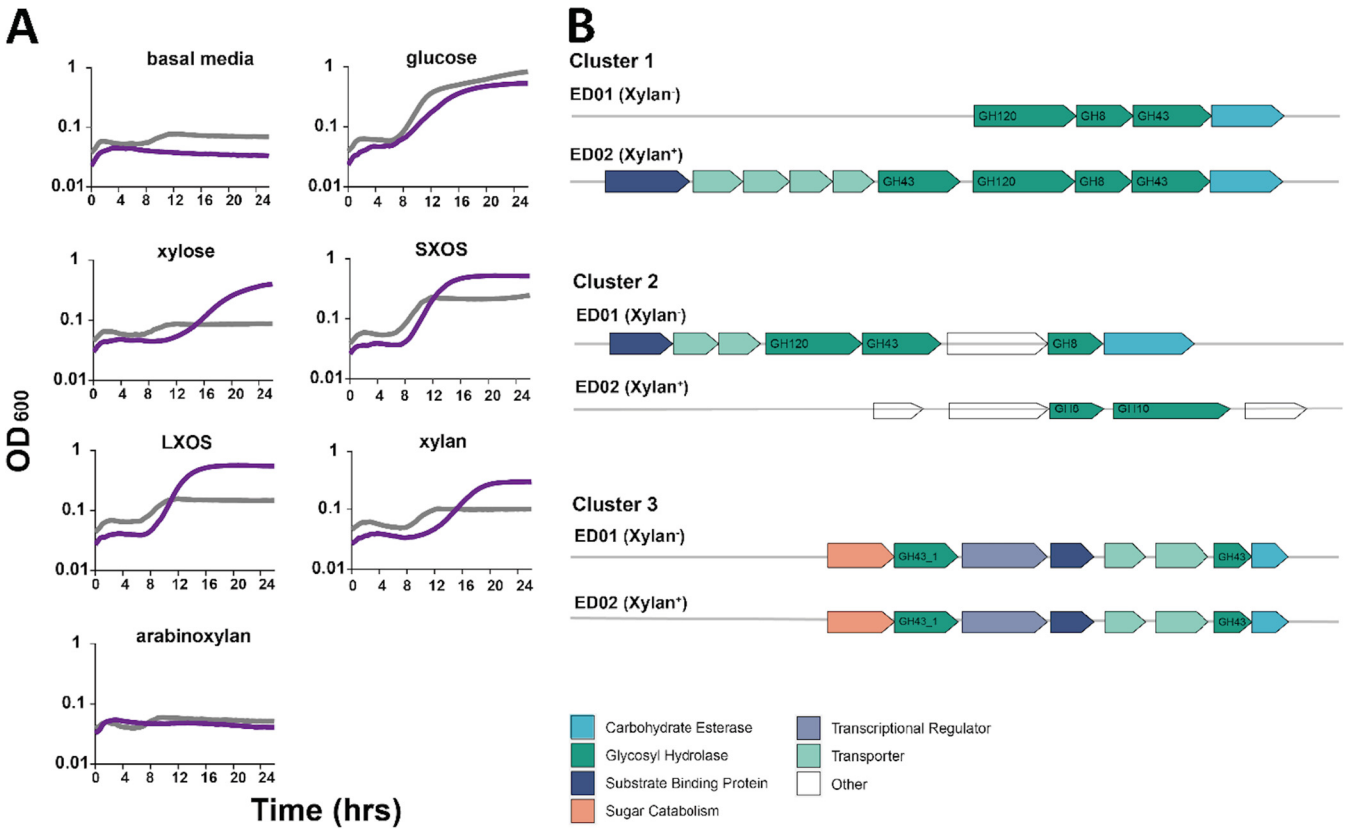

FIG 1 Differences in growth phenotypes and XOS-active gene clusters between xylan$^+$ ED02 and xylan$^-$ ED01 *B. pseudocatenulatum* strains. (A) Growth of *B. pseudocatenulatum* xylan$^+$ strain ED02 (purple) and xylan$^-$ strain ED01 (gray) on various xylose-based carbohydrates. Cells were grown in modified deMan, Rogosa, and Sharpe (mMRS) medium supplemented with 0.5% carbohydrate. Basal medium, with no added carbohydrate, was used as a negative control, and glucose was used as a positive control. Other carbohydrate treatments included xylose, short-chain XOS (enriched in DP less than 4), long-chain XOS (enriched in DP greater than 4), xylan, and arabinoxylan. (B) Presence of XOS-active gene clusters between xylan$^+$ and xylan$^-$ phenotypes. Genes encoding XOS-active clusters I, II, and III are aligned according to their phenotype and are color-coded for relevant carbohydrate-active functions.

genes that were orthologous to the substrate binding protein, multiple transporter genes, and one glycosyl hydrolase gene (GH43).

Additionally, cluster II was found to be present only in the xylan$^-$ strains ED01 and CR16 and absent in ED05, while the xylan$^+$ strains ED02 and ED03 harbor a homologous reducing-end xylose-releasing exo-oligoxylanase gene (GH8). Interestingly, a putative extracellular GH10 endo-β-1,4- xylanase gene was located adjacent to the GH8 xylanase gene present in the ED02 and ED03 genomes. Collectively, these results suggest that the extracellular GH10 gene is important for xylan metabolism and confirm that the presence or absence of key glycosyl hydrolases and transport systems is consistent with the observed phenotypes.

A pangenome analysis with 86 *B. pseudocatenulatum* genomes from the NCBI database and 5 genomes from this study was conducted to further investigate the prevalence of these XOS-associated genes and CGCs in the *B. pseudocatenulatum* species. This analysis revealed the presence of 5,620 genes consisting of 1,227 core genes (present in all 86 genomes), 2,965 shell genes (present in 2 to 85 genomes), and 1,428 cloud genes (present in only one genome). Among these genomes, only 19 contained a GH10-encoding gene, including the two xylan$^+$ strains in this study (Fig. S2). In addition, these results indicated differences in the prevalence of each XOS-active gene cluster in *B. pseudocatenulatum* species. For example, cluster III was highly conserved and was found to be present in all strains. Cluster I was the second most prevalent, with 64 of 86 genomes containing the complete cluster, followed by cluster II, which was found to be complete in 33 of the 86 genomes (Fig. S2A). However, the GH8 reducing-end xylose-releasing exo-oligoxylanase gene was found to be present in 50 of the 86

genomes. This includes all 19 genomes where the GH10-encoding gene was present as observed in the xylan$^+$ ED02 and ED03 strains (Fig. S2B).

To investigate the prevalence of GH10 in other *Bifidobacterium* genomes, 1,355 *Bifidobacterium* genomes from NCBI RefSeq were screened for the presence of GH10 xylanases. This analysis revealed that a GH10 xylanase-encoding gene was found to be present in only 29 genomes (2.14%), including 17 *B. pseudocatenulatum*, 4 *B. catenulatum*, 3 *B. pullorum*, and 2 *B. adolescentis* strains. Single genomes from *B. reuteri*, *Bifidobacterium animalis* subsp. *lactis*, and one *Bifidobacterium* species were also found to contain a GH10 xylanase gene (Fig. S3).

Biochemical evidence of xylan utilization and cross-feeding. Both *in vitro* growth experiments and *in silico* genome analysis indicated that the xylan$^+$ phenotype was dependent on a putative extracellular xylanolytic system. To confirm the presence of an extracellular xylanase, cell-free supernatants were obtained from all five representative strains. When MRS broth containing LXOS was supplemented with these supernatants and assessed by thin-layer chromatography (TLC), hydrolysis products ranging from DP2 to D4 were observed only for the ED02 or ED03 supernatants (Fig. 2A). The same activity was also observed on xylan, where only the xylan medium inoculated with the xylan$^+$ supernatant resulted in xylan hydrolysis products (Fig. 2B). When the supernatant was heat treated, no hydrolysis products were formed, confirming that hydrolysis was due to the presence of extracellular xylanases.

The presence of an ED02 xylanase and its activity on XOS and xylan were also demonstrated by high-performance liquid chromatography (HPLC) analysis of hydrolysis products. The results indicated an increase in the concentration of DP2 -4 XOS products, similar to the TLC results. In addition, HPLC revealed a decrease in DP5 -13 XOS fragments from the xylanase-treated LXOS, as well as production of DP2 -6 products from xylan (Fig. 2C; Fig. S4). When this medium was then inoculated with the xylan$^-$ strain ED01, enhanced growth on both substrates was observed (Fig. 2D).

Persistence of strains in fecal fermentation is consistent with phenotypes in pure culture. Fecal fermentations across all three xylose-based substrates combined with either strain ED01 or ED02 were performed to test for strain persistence within a complex fecal community. Persistence of strains during these stepwise fecal fermentations containing five different donor samples was consistent with their xylan and LXOS phenotypes. Xylan$^+$ strain ED02 persisted on LXOS for all five donor samples (Fig. 3D) and on xylan for four of the five donor samples (Fig. 3F) but was displaced during growth in basal medium (Fig. 3B). In contrast, strain ED01 was displaced in fermentations containing LXOS or xylan as well as the basal fermentations (Fig. 3A, C, and E).

Samples at baseline and at the 72-h time point for the five fecal-fermentation samples were sequenced via 16S rRNA amplicon sequencing to assess changes in the microbial community. For all samples at 72 h, significant decreases in alpha diversity (Shannon index) were observed compared to baseline samples ($P < 0.05$) (Fig. 4A). Similarly, alpha diversity of all substrate-only fermentations was significantly different from baseline, presumably because the method also selects for taxa resistant to dilution pressure (Fig. 4B). Additionally, the XOS treatment was significantly less diverse than the basal treatment. ($P < 0.01$). Beta diversity was evaluated using principal-coordinate analysis (PCoA) based on Jaccard distance to compare differences in community composition between substrate treatments (Fig. 4C). As expected, the fecal baseline clustered distinctly from the substrate treatments. Interestingly, the XOS-treated fermentation samples also clustered separately from the basal treatment, while the xylan-treated samples overlap between the two.

Bifidobacterium was detected in all five fecal baseline samples and was initially present at greater than 5% relative abundance in subjects A33 and A35 (Fig. S5). After 72 h of stepwise growth in basal fecal-fermentation medium with no added carbohydrates, the relative abundance of *Bifidobacterium* decreased for both ED01 and ED02 treatments, as well as fermentations with no added strain. Based on differential analysis comparing basal fecal-fermentation samples at baseline to those at 72 h, a method effect was apparent. Specifically, there were consistent increases in various fast-growing taxa,

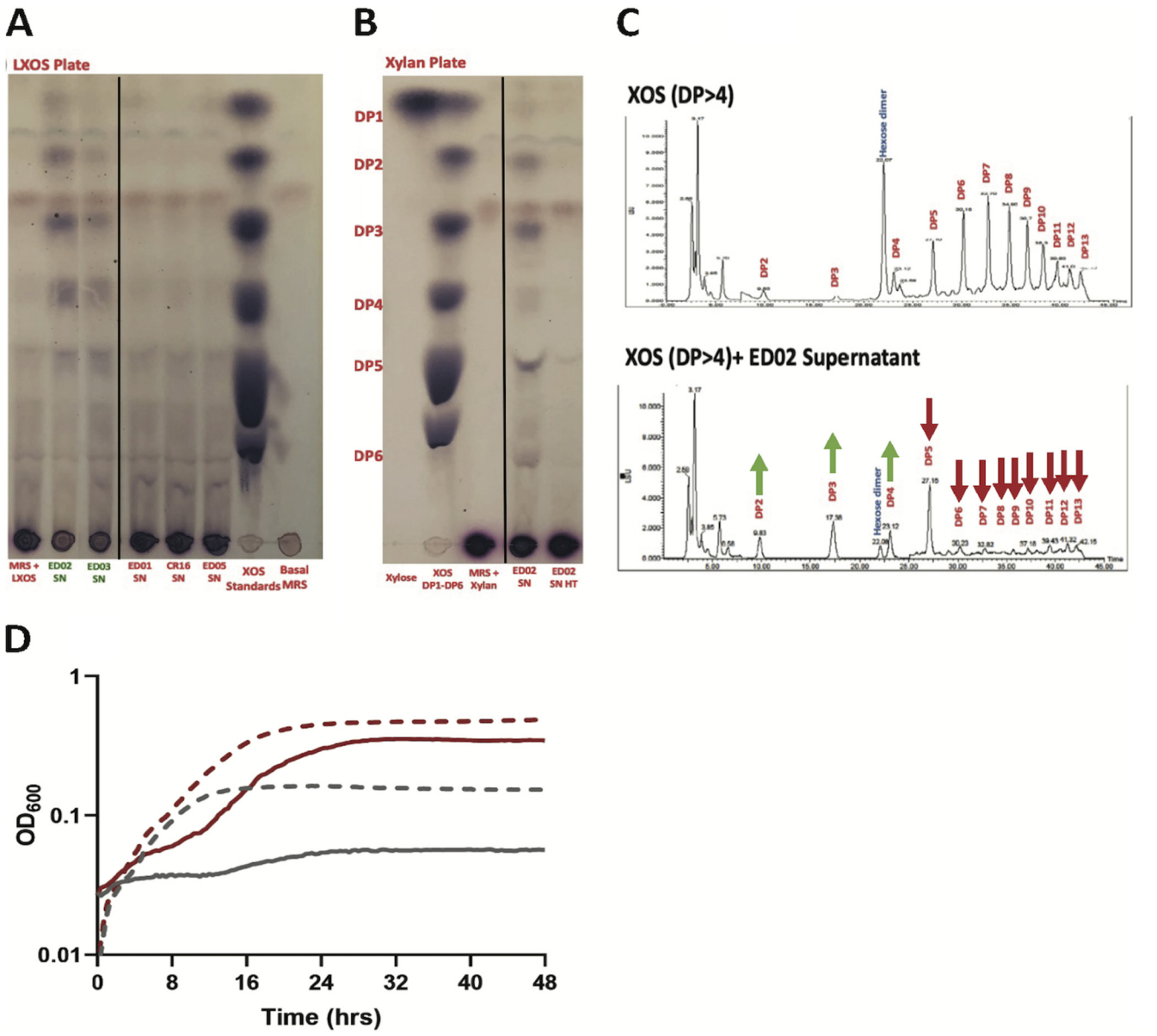

FIG 2 Production of endoxylanase and extracellular xylanase in *B. pseudocatenulatum* ED02 supports cross-feeding relationships between xylan$^+$ and xylan$^-$ strains. Shown are thin-layer chromatography (TLC) results of supernatant inoculated media containing either LXOS (lane 1, LXOS medium; lanes 2 to 6, LXOS media inoculated with respective strain supernatant; lane 7, 15 mM XOS standards DP1 to DP6; lane 8, basal medium) (A) or xylan (lane 1, xylose; lane 2, 15 mM XOS standards DP1 to DP6; lane 3, xylan medium; lane 4, xylan medium inoculated with ED02 supernatant; lane 5, xylan medium inoculated with heat-treated ED02 supernatant) (B). The chromatograms are composite of lanes from the same TLC plate. (C) Growth of xylan$^-$ strain ED01 in the presence (red) or absence (gray) of ED02 supernatant-inoculated LXOS (dashed line) and xylan (solid line). (D) High-performance liquid chromatography (HPLC) indicates endoxylanase activity by ED02 producing small XOS fractions. Degradation products by ED02 supernatants after 48 h of incubation with XOS were separated and quantified by HPLC. In the XOS media, DP2 to -4 increased and DP5 to -13 decreased. Trends are indicated by arrows, displaying change in area under the curve from time zero to 48 h.

including amplicon sequence variants (ASVs) from the genera *Escherichia-Shigella*, *Enterococcus*, *Streptococcus*, and *Fusobacterium* (Fig. S5 and S6). Other method effects included significant decreases in several fiber-associated bacteria, including *Roseburia*, *Akkermansia*, and *Prevotella* (Fig. S6).

Bifidobacterium was enriched with XOS supplementation for two (A33 and A35) of the five donor samples even in the absence of an inoculated strain (Fig. S5). Relative abundances of *Bifidobacterium* also increased in all subjects when fecal fermentations were inoculated with strains ED01 and ED02. Three *Bifidobacterium* ASVs were identified from the fecal fermentations and were assigned as *B. pseudocatenulatum*, *B. adolescentis*,

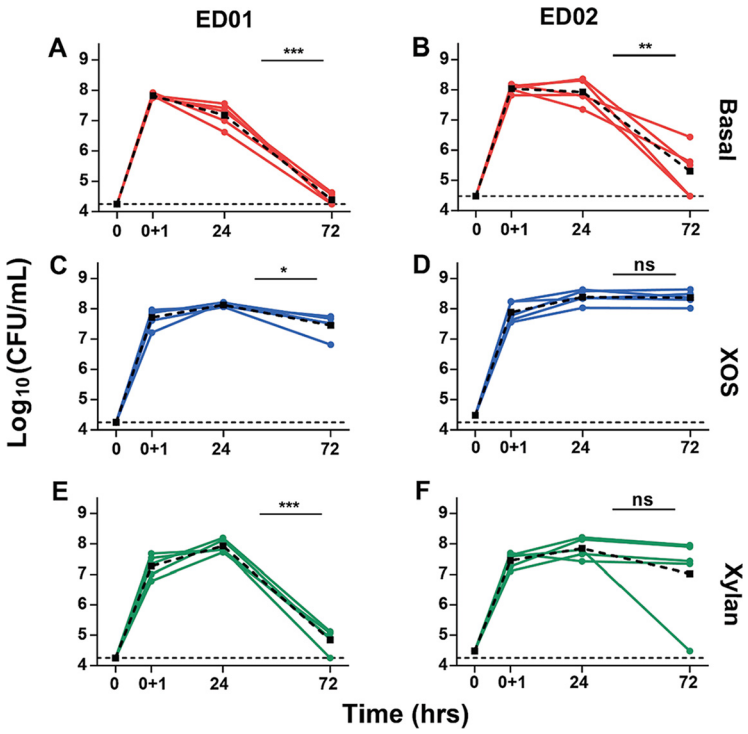

FIG 3 Test of persistence of *B. pseudocatenulatum* strains in fecal fermentations. Shown is qPCR quantification of strains ED01 and ED02 on basal medium (A and B), XOS (C and D), and xylan (E and F) in fecal fermentations with samples from 5 subjects. Persistence in individual fecal samples is shown as solid lines with colored circles, and averages are shown as dashed lines with square symbols. Significant differences between 24 h and 72 h were determined using a repeated-measure mixed model (*, $P < 0.05$; **, $P < 0.01$; ***, $P < 0.001$).

and *B. longum* according to sequence similarity and the number of species-specific taxonomic hits against the NCBI nonredundant (nr) database (Table S3). The *B. pseudocatenulatum* ASV increased significantly in both ED01 and ED02 supplemented XOS media, while significant increases in the other two *Bifidobacterium* ASVs were not observed in the presence of XOS.

On xylan, the relative abundance of *Bifidobacterium* for all five subjects in both the control treatment and ED01 treatment decreased by the 72-h time point, accompanied by an observed decrease in two *Bifidobacterium* ASVs (*B. adolescentis* and *B. longum*) from the differential abundance analysis (Fig. S5 and S6). In the ED02 treatment with xylan, there was an increase in relative abundance of *Bifidobacterium* in subjects A31, A33, A34, and B39 but a decrease in subject A35. However, no significant change in any *B. pseudocatenulatum*-associated ASV was observed from the differential-abundance analysis (Fig. S6). Instead, a significant reduction was observed for a *Bifidobacterium* ASV (*B. adolescentis*) that was present at baseline.

DISCUSSION

The importance of xylans as dietary substrates for gut microbes has led researchers to identify and characterize strains having the biochemical and genetic means to metabolize these carbohydrates (14, 19, 27). In this study, two major xylan phenotypes were observed among strains of the human gut-residential species *B. pseudocatenulatum*. Strains having a xylan$^+$ phenotype were considered primary degraders, hydrolyzing xylan via an extracellular GH10 xylanase and forming XOS fractions of various DPs. This is consistent with the activity of GH10 xylanases described previously (28–30). Furthermore, growth of the xylan$^+$ strain ED02 directly on xylan, as well as LXOS, indicated this strain could also consume small- and large-DP hydrolysis products. Comparative genome analysis of the *B. pseudocatenulatum* strains revealed the presence of three XOS-

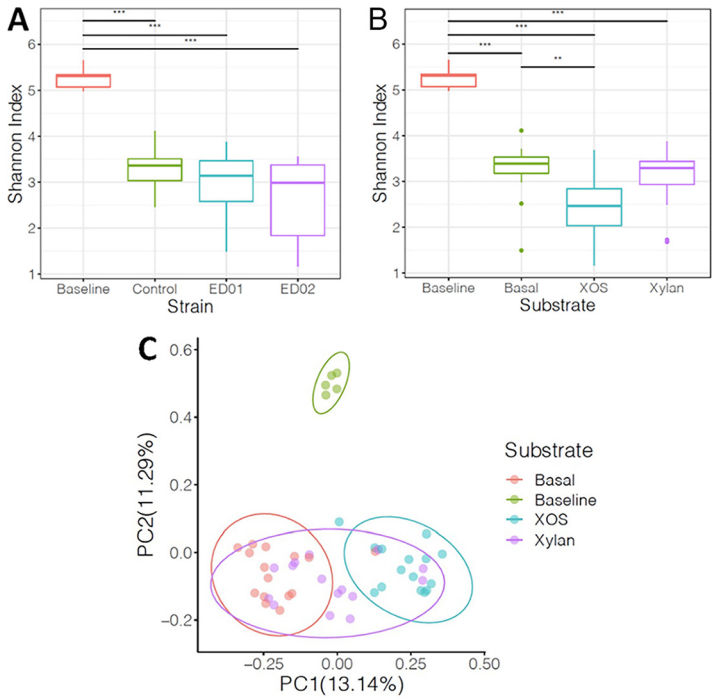

FIG 4 Analysis of microbial diversity and community composition through 16S rRNA sequencing of fecal fermentations at baseline and 72 h. (A and B) Shannon index was used to measure alpha diversity, and comparisons were made between strain (A) and substrate (B) treatments with baseline and respective controls. Significant differences are indicated by asterisks (Wilcoxon rank sum test with false-discovery rate [FDR] correction; *, $P < 0.05$; **, $P < 0.01$; ***, $P < 0.001$). (C) Beta diversity between substrates was visualized by principal-coordinate analysis (PCoA) based on Jaccard Index. Ellipses indicate 95% confidence intervals.

associated clusters, consistent with those described previously (27). In this study, both cluster I and cluster III were present in xylan$^+$ strains and contained substrate binding proteins with predicted affinities for LXOS and SXOS, respectively. In addition, the GH8, GH43, and GH120 glycoside hydrolases present in these XOS-active clusters are likely used to degrade intracellular XOS into xylose.

In contrast to ED02, which was a primary degrader as well as consumer of xylan, other strains had a xylan$^-$ phenotype but could still grow on XOS. These strains were considered secondary consumers. Thus, in complex communities where xylans are hydrolyzed by primary degraders, secondary consumers obtain substrates via cross-feeding (Fig. 5) (11, 14). This was demonstrated by enhanced growth of strain ED01 on LXOS and xylan in the presence of the extracellular xylanase produced by ED02. These xylan$^-$ strains likely employ the same XOS transport systems encoded in cluster III as xylan$^+$ strains, since this cluster is highly conserved in *Bifidobacterium* (27). Moreover, the possibility that exchange of these genes occurs more frequently among populations who frequently consume xylan or other nondigestible carbohydrates has recently been proposed (31).

Interestingly, we observed that all strains examined in this study grew better on XOS than on xylose. *Bifidobacterium* organisms are well known to have adapted to the gut environment, where simple sugars are absent and oligosaccharides, including XOS, are more abundant. For example, *B. adolescentis* was shown to have higher specific growth rates on fructooligosaccharides than on fructose (32). Likewise, a strain of *Bifidobacterium longum* subsp. *infantis* was shown to grow better on human milk oligosaccharides than on glucose (33). These findings strongly support the evolutionary adaptation of *Bifidobacterium* to grow on a range of oligosaccharides which is reflected by the presence of relevant transporters and associated transport machinery in their genomes (34–36).

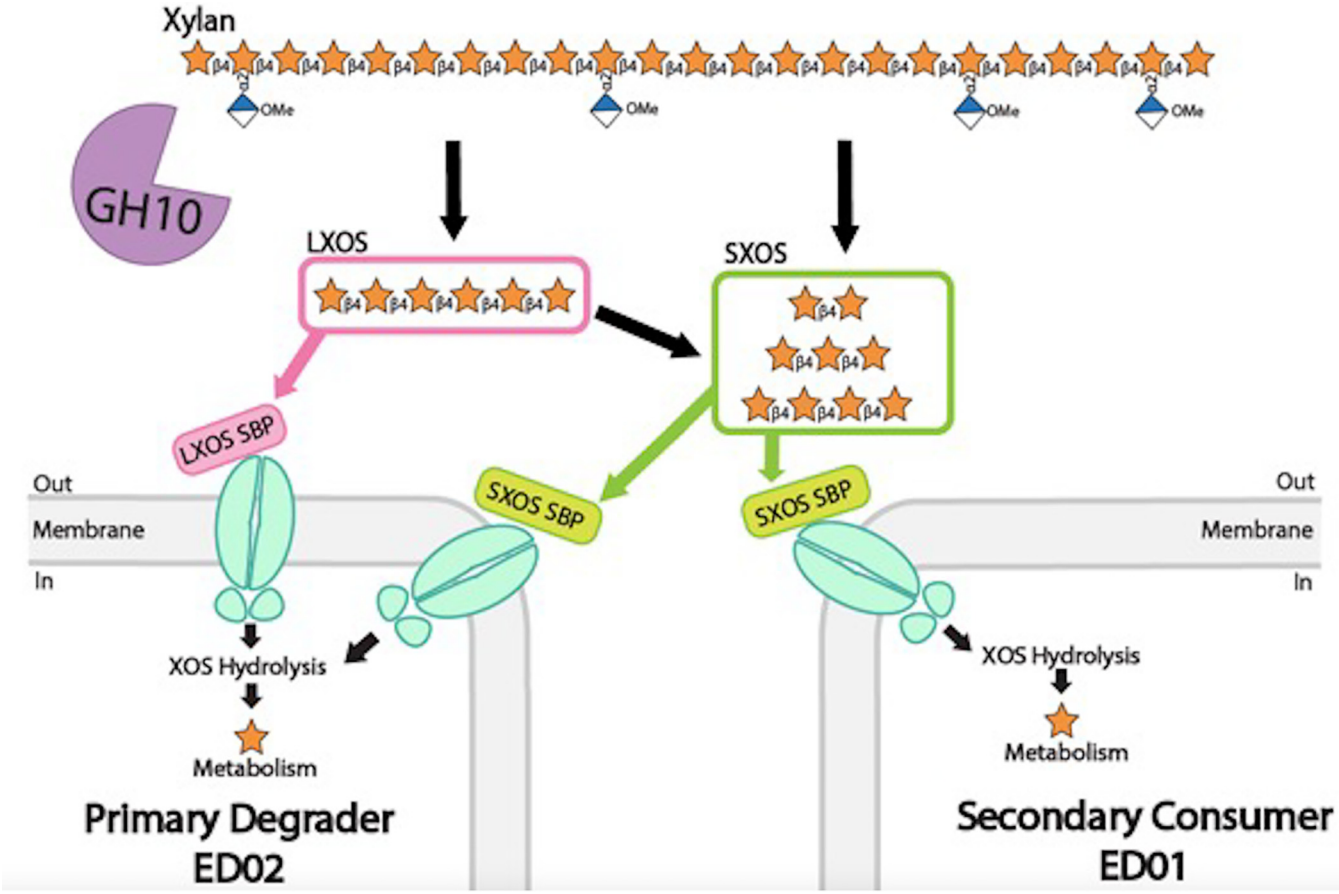

FIG 5 Model for xylan and XOS utilization by *B. pseudocatenulatum*. The xylan$^+$ phenotype is implicated as a primary degrader due to the secretion of an extracellular xylanase that degrades xylan into smaller oligomers. The latter are available for transport by the primary degrader, or they can cross-feed other organisms. In contrast, strains having a xylan$^-$ phenotype may still be secondary consumers. Such strains do not have the extracellular enzymatic machinery or transporters to consumer larger XOS and xylan molecules; they instead rely on other members of the microbial community to degrade xylans into smaller oligosaccharides that can serve as substrates for relevant transporters.

Recently, other investigators reported the presence of a XOS cluster containing GH8 and GH10 xylanases in *B. pseudocatenulatum*, although as in our study, this cluster was only present in a portion of the strains examined (12, 37). In one study (37), which surveyed a total of 217 strains of *Bifidobacterium* from six human-origin species, the GH10 xylanase was found in only 9 of 30 *B. pseudocatenulatum* strains and was absent in all other *Bifidobacterium* strains. Moreover, in another recent study, despite the presence of 30 glycoside hydrolase families, GH10 xylanases were not detected in any of the 88 strains of *B. pseudocatenulatum* examined (38). From our *in silico* analyses, putative GH10 xylan-containing species also include *B. catenulatum*, *B. adolescentis*, *B. pullorum*, *B. animalis* subsp. *lactis*, and *B. reuteri*. In particular, *B. catenulatum* and *B. adolescentis*, along with *B. pseudocatenulatum*, belong to the *B. adolescentis* phylogenetic group that are considered adult-type bifidobacteria (39). Thus, the ability of these strains to metabolize xylan would be consistent with the consumption of dietary fiber in the adult human diet (18, 19).

In another recent study, 12 of 35 *B. pseudocatenulatum* strains harbored a GH10 xylanase and also grew on long-chain xylan as well as wheat arabinoxylan as a carbohydrate substrate (12). This arabinoxylan growth phenotype was not observed in our study, which may be attributed to the use of corn arabinoxylan, a more complex substrate than wheat arabinoxylan. Previous studies suggest that corn arabinoxylans are indeed more resistant to xylanase hydrolysis (40, 41). Thus, it is possible that the strains used in our study may have had a similar phenotype on wheat arabinoxylans as the strains used in the previous study (12).

The ability of *B. pseudocatenulatum* ED02 to grow on xylan or LXOS likely provides a

TABLE 2 Substrates used in this study

Substrate	Label	Supplier	Composition
SXOS	XOS-NUSR	Prenexus Health	Short-chain XOS; enriched in DPs of <4
LXOS	XOS-NUSP	Prenexus Health	Long-chain XOS; enriched in DPs of >4
PreneXOS	PreneXOS	Prenexus Health	Mixture of XOS and xylan
Xylan	Xylan (Beechwood)	Megazyme	Glucuronoxylan from beechwood
Arabinoxylan	AgriFiber BFG	AgriFiber	Soluble prebiotic corn bran fiber; DP17 to -24
Xylose	D-(+)-xylose	Sigma	Xylose
Glucose	D-(+)-glucose	Sigma-Aldrich	Glucose

competitive advantage in mixed cultures or complex environments containing XOS as the carbohydrate source. However, xylan$^-$ strains also benefitted from the activity of xylan$^+$ strains. That one strain supports growth of another strain within the same ecosystem by degrading xylan-rich substrates suggests that cross-feeding and cooperation exist within the *B. pseudocatenulatum* group, similar to what has been described for *Bacteroides* during growth on glucose and fructose polysaccharides as well as xylan-type polysaccharides (14, 42). In our study, the observation of within-species cooperation was further supported by the *in vitro* stepwise fecal fermentations. Although ED01 failed to persist with xylan as a substrate, this strain persisted on XOS, suggesting that if primary xylan degraders were present, secondary XOS consumers would have sufficient substrate to grow and persist.

Collectively, our findings extend previous reports on the role of *B. pseudocatenulatum* in the degradation and utilization of xylan and xylan-derived oligosaccharides. We provide biochemical evidence for a GH10 xylanase produced by human-origin *Bifidobacterium* and showed that these strains can cross-feed non-GH10-producing strains of the same species. Thus, cooperative utilization of xylan among different strains of *B. pseudocatenulatum* suggests that resource sharing, a trait common to bifidobacterial communities (43), can also occur within a single species.

MATERIALS AND METHODS

Isolation and identification of *Bifidobacterium* isolates. Fifteen putatively unique *Bifidobacterium* isolates from five adult subjects were used in this study. These isolates had been previously obtained (26) from *in vitro* fecal enrichment fermentations with 1% XOS (Prenexus Health, USA) and presumptively identified as *B. pseudocatenulatum* by 16S rRNA sequencing. To confirm species identity, DNA was extracted with a QIAamp DNA minikit (Qiagen, USA), and quantitative PCR (qPCR) was performed using *B. pseudocatenulatum*-specific primers (44). One isolate from each subject was selected as the representative strain for further genomic and functional analysis. These strains were renamed ED01, ED02, ED03, CR16, and ED05. In addition to the *B. pseudocatenulatum* isolates, 11 other *Bifidobacterium* strains were assessed for their ability to utilize xylose-based glycans.

Growth characteristics of *Bifidobacterium* strains and isolates. To characterize the ability of *B. pseudocatenulatum* strains to utilize xylose-based glycans, growth studies were performed in modified de Man, Rogosa, and Sharpe media (mMRS) in which glucose was replaced with various carbohydrates (Table 2). Strains were first grown on MRS plates for 48 h, and single colonies were inoculated into MRS broth and incubated anaerobically at 37°C for 24 h in a Sheldon Bactron IV-900 anaerobic chamber (Cornelius, OR, USA). Cells were then transferred into MRS, and overnight cultures were used to inoculate mMRS containing 0.5% carbohydrate. Growth experiments were performed in quadruplicate, with a final volume of 200 μL, in 96-well microplates. Plates were incubated anaerobically, and optical density measurements (600 nm) were obtained every 20 min using a Tecan (Männedorf, Switzerland) Sunrise microplate reader until stationary phase was reached.

Growth phenotypes of other *Bifidobacterium* species on xylose-based substrates were determined by growth in mMRS containing xylan, LXOS, or xylose at a 1% concentration. Experiments were performed, in triplicate, in 200-μL microwell volumes, and phenotypes were based on growth and pH. Xylan and XOS DP2 to -6 standards were obtained from Neogen Megazyme (USA), and SXOS and LXOS were obtained from Prenexus Health.

DNA extraction. Genomic DNA from isolated strains and for pure culture experiments was extracted with the QIAamp DNA minikit using the manufacturer's protocol for Gram-positive bacteria (Qiagen, Hilden, Germany). For fecal-culture experiments, DNA was extracted using BioSprint 96 One-For-All Vet kits (Qiagen) according to the manufacturer's protocol, with modifications as described previously (45). Sample concentrations were quantified using a NanoDrop ND-1000 spectrophotometer.

Whole-genome sequencing, assembly, and annotation. Whole-genome sequencing of the five selected *B. pseudocatenulatum* strains was performed by the Microbial Genome Sequencing Center (MiGS).

Raw read sequences were checked for read quality using FastQC (46), and the sequences were trimmed using Sickle to remove low-quality reads (47). The reads were assembled into contigs and scaffolds using SPAdes (48). Scaffolds were aligned using Mauve against the reference genome *B. pseudocatenulatum* 12 retrieved from the NCBI database (49). The assembled genomes were annotated using Prokka (50). A summary of features for each strain is shown in Table S2. Additional annotations against the carbohydrate-active enzyme (CAZy) database were obtained using dbCAN2 to identify CAZy clusters (51).

***B. pseudocatenulatum* pangenome analysis.** Pangenome analysis was performed using 86 *B. pseudocatenulatum* genomes. The genomes included those of the 5 strains reported here and 81 additional *B. pseudocatenulatum* genomes from the Prokaryotic RefSeq Genomes database in NCBI (52). Pangenomic analyses were performed with anvi'o with the MCL (Markov cluster) algorithm using an inflation parameter of 10 to identify and cluster amino acid sequences between genomes (53, 54). Further annotations were performed using dbCAN2 to identify prevalence of XOS active clusters in the *B. pseudocatenulatum* pangenome (51).

Prevalence of GH10 xylanase in *Bifidobacterium*. To determine the prevalence of GH10 xylanases in *Bifidobacterium*, 1355 nonredundant *Bifidobacterium* genomes were obtained from the Prokaryotic RefSeq Genomes database from NCBI (52). These genomes were annotated with three CAZy databases, HMMER, DIAMOND, and Hotpep, using the dbCAN2 metaserver (51, 55–57). A genome was considered to contain GH10 if at least two CAZy databases concurred. Species level associations were then assigned.

Assessing enzymatic activities. To determine if extracellular enzymes capable of hydrolyzing XOS or xylan were secreted, cell-free supernatants were obtained from spent XOS cultures. Strains were grown anaerobically at 37°C in mMRS supplemented with 1% LXOS in 10-mL volumes for 24 h. Cultures were centrifuged (Eppendorf AG, Hamburg, Germany) at 3,100 $\times$ *g* for 10 min. Supernatants were collected, filter sterilized through a 0.22-μm filter, and divided into aliquots. One aliquot was used directly (see below), and the second was heat treated at 95°C for 5 min to inactivate enzymes.

Identification of hydrolysis products. Basal mMRS containing 1% xylan or 1% LXOS was supplemented with 20% supernatant that was either heat treated or not heat treated. Samples were obtained at time zero and after 48 h of incubation at 37°C. All samples were then heat treated, as described above, to halt further enzymatic activity and then stored at −20°C. Identification of hydrolysis products was done using high-performance thin-layer chromatography silica gel 60 (Sigma-Aldrich, St. Louis, MO), as described previously (26). Briefly, plates were spotted with 8.5 μL of medium and supernatant-inoculated medium and 5 μL of standards, including 2% xylose and 10 μM XOS DP1 to -6 standards (Neogen Megazyme). Plates were developed in solvent containing 1-butanol–2-propanol–H_2O (3:12:4), sprayed with 0.5% α-naphthol and 5% H_2SO_4, and heated at 80°C for 30 min.

Selected samples were also analyzed by high-performance liquid chromatography (HPLC) at the National Renewable Energy Laboratory (NREL). The HPLC system included a Waters Acquity ultraperformance LC (Waters Co., Milford, MA, USA) coupled with a mass spectrometer (MS) and an evaporative light scattering detector. The system ran with a Shodex sugar SZ5532 (zinc) column (Showa Denko K.K., Japan) at 6 by 150 (mm), 6-μm particle size, using a ramped mobile phase of acetonitrile and water with 0.1% formic acid with a flow rate of 0.9 mL min^{-1} and a column temperature of 60°C. DP fractions were identified via molecular weight and retention time from standards. Detector responses recorded enzymatic action observed by changes in area under the chromatogram curves from baseline to 48 h.

Coculture simulation of *B. pseudocatenulatum* strains. To assess if cross-feeding was occurring between strains, growth curves were performed using the enzymatic supernatants described above. Supernatants were added at 20% to fresh medium containing 1% LXOS or xylan. The medium was then inoculated with xylan-non-fermenting strains and incubated for 48 h.

***In vitro* establishment of *B. pseudocatenulatum* strains.** Fecal samples were obtained from five volunteers following UNL institutional board review (IRB) protocols (no. 20160616139). Inclusion criteria included the following: age of at least 19 years, no known history of gastrointestinal diseases, no consumption of antibiotics or probiotics in the previous 6 months, and no regular consumption of yogurt. The fecal samples were then homogenized and stored in phosphate-buffered saline (PBS; pH 7.0), as previously described (26).

Sterile fecal-fermentation medium containing 0.5% LXOS or xylan or no added carbohydrate was made as described previously (58). The test of persistence was performed in stepwise fecal fermentations as described previously (21). Briefly, fecal slurries were diluted in PBS in a 1:10 ratio and added to the fermentation medium in a 3:6 (vol/vol) ratio in a total volume of 9.0 mL. Then, *B. pseudocatenulatum* strains ED01 and ED02, grown as previously described, were inoculated at 10^7 CFU/mL into the fecal-fermentation medium. The fermentations were incubated anaerobically at 37°C, with subsequent dilutions performed in microplate format by transferring 10 μL into 990 μL of fresh fermentation medium every 24 h. This process was repeated three times, with samples collected at time zero and 24, 48, and 72 h. DNA was extracted to assess persistence by qPCR. Samples were also used for 16S rRNA sequencing.

Design of strain-specific primers. Strain-specific primers were designed using RUCS (rapid identification of PCR primers for unique core sequences) (59). All five isolated *B. pseudocatenulatum* genomes and two complete *B. pseudocatenulatum* genomes from the NCBI genome database were used to identify unique target sequences. Primer specificity was confirmed using NCBI Primer BLAST against the NCBI RefSeq representative genome database for bacteria. No primers were accepted that gave hits for species present in human fecal samples. Primer annealing temperatures were identified using a gradient PCR program, and primer specificity was confirmed by performing qPCR against all other *B. pseudocatenulatum* strains isolated.

TABLE 3 PCR conditions and sequences used to target different *Bifidobacterium* groups in this study

Target organism	Primer		Annealing temp (°C)	Reference
	Direction	Sequence (5′ → 3′)		
B. pseudocatenulatum ED01	Forward	CAG CCA AGA ACA CAC TGC	62	This study
	Reverse	GCA TGG CAA CTG TCT TCG TTT		
B. pseudocatenulatum ED02	Forward	GCA GGT CAG AAT GTG AGA CGA	62	This study
	Reverse	CGA ACC TCT GTC CAA CGA TGA		
B. pseudocatenulatum ED03	Forward	CTT GCT GGG AGA AGT CGT CTT	62	This study
	Reverse	TCG ATT TGT TCC GTT CGT		
B. pseudocatenulatum CR16	Forward	AAG GCT CGT GTT ATC CGG TTT	62	This study
	Reverse	GCG CTT CGA AAT CCT GTG TAC		
B. pseudocatenulatum ED05	Forward	CGA TTC GAC AAC ACG TAC ACG	62	This study
	Reverse	TCA GAT GTT TGT CCG CTT CGA		
B. pseudocatenulatum	Forward	AGC CAT CGT CAA GGA GCT TAT CGC AG	68	44
	Reverse	CAC GAC GTC CTG AGA GCT CAC		
Bifidobacterium	Forward	TCG CGT CYG GTG TGA AAG	68	26
	Reverse	CCA CAT CCA GCR TCC AC		

Quantification using quantitative real-time PCR. To determine persistence of specific strains and total *Bifidobacterium* in fecal fermentations on different substrates, qPCR was performed using strain-specific and genus-specific primers (Table 3). Quantitative PCR was performed using these primers with the Mastercycler Realplex2 (Eppendorf AG, Hamburg, Germany). The qPCR master mix contained 12.5 μL of SYBR green (Thermo Fisher Scientific, MA, USA), 0.5 μL of forward primer, 0.5 μL of reverse primer, 10.5 μL of DNA-grade water, and 1 μL of sample, in a total volume of 25 μL per reaction. The qPCR conditions were as previously described (44).

Persistence of strains on respective substrates was analyzed using a repeated-measure mixed model. This model relegates subject as the random effect, while prebiotic and time are fixed effects. Persistence was measured as the $\log_{10}$ difference in CFU per milliliter of strains between the 24- and 72-h samples. Calibration curves for strain-specific growth were obtained using diluted DNA samples collected from pure culture growth on modified MRS of ED01 and ED02, respectively. Analysis was performed using SAS v.9.4, and *P* values were adjusted with Tukey adjustment.

16S rRNA amplicon sequencing and analysis. Sequencing of the V4 region of the 16S rRNA gene was carried out as described previously on an Illumina MiSeq platform with paired-end sequencing of 250 bp (26, 60). Fecal-fermentation samples at the 72-h time point and the five fecal baselines were selected for analysis. A total of 1,292,111 sequences were obtained, with a mean of 25,335 sequences per sample (maximum, 73,706; minimum, 7,061).

Sequence processing was performed using the DADA2 pipeline within QIIME2 2017.4 (61, 62). Raw sequence data were demultiplexed and denoised to remove chimeric sequences, and forward and reverse reads were trimmed to 220 bp and 160 bp, respectively. Amplicon sequence variants (ASVs) were inferred and taxonomy was assigned using the SILVA 16S database (63). To further refine output, samples with fewer than 1,500 reads and ASVs with fewer than 15 reads were removed.

Statistical analysis and visualization of community sequencing data were done in QIIME2 2017.4 and RStudio (v.4.0.0). Alpha diversity was measured via the Shannon index and compared via a Wilcoxon rank sum test. Beta diversity was visualized using a principal-coordinate analysis (PCoA) plot of the Jaccard index with 95% confidence interval ellipses for the respective treatments. Changes in microbial composition from baseline to 72 h were visualized by $\log_2$ fold change of specific ASVs with a significance cutoff of *P* value <0.05 using DESeq2.

Data availability. Whole-genome sequences and 16S rRNA sequences have been submitted to GenBank under BioProject PRJNA820700.

SUPPLEMENTAL MATERIAL

Supplemental material is available online only.

SUPPLEMENTAL FILE 1, PDF file, 2 MB.

ACKNOWLEDGMENTS

We thank Ed Wolfrum and Bill Michener from the National Renewable Energy Laboratory (NREL) for HPLC analysis of XOS hydrolysis products. We thank Prenexus Health for providing XOS and AgriFiber Solutions for providing AXOS. We also thank Nathaniel Korth for assistance with 16S rRNA sequencing and David Gomez for help in statistical analysis of fermentation samples.

C.R.K. was supported by a Nebraska Food for Health Center Fellowship. R.H. has received grants and honoraria from several food and ingredient companies, is a co-owner

of Synbiotic Health, and was on the board of directors of the International Scientific Association for Probiotics and Prebiotics.

REFERENCES

1. Bajpai P. 2014. Xylanolytic enzymes. Elsevier Inc, Amsterdam, The Netherlands.
2. Faik A. 2010. Xylan biosynthesis: news from the grass. Plant Physiol 153:396–402. https://doi.org/10.1104/pp.110.154237.
3. Broxterman SE, Schols HA. 2018. Characterisation of pectin-xylan complexes in tomato primary plant cell walls. Carbohydr Polym 197:269–276. https://doi.org/10.1016/j.carbpol.2018.06.003.
4. Zhan P, Ye J, Lin X, Zhang F, Lin D, Zhang Y, Tang K. 2020. Complete genome sequence of *Echinicola rosea* JL3085, a xylan and pectin decomposer. Mar Genomics 52:100722. https://doi.org/10.1016/j.margen.2019.100722.
5. Jia X, Mi S, Wang J, Qiao W, Peng X, Han Y. 2014. Insight into glycoside hydrolases for debranched xylan degradation from extremely thermophilic bacterium *Caldicellulosiruptor lactoaceticus*. PLoS One 9:e106482. https://doi.org/10.1371/journal.pone.0106482.
6. Dodd D, Moon Y-H, Swaminathan K, Mackie RI, Cann IKO. 2010. Transcriptomic analyses of xylan degradation by *Prevotella bryantii* and insights into energy acquisition by xylanolytic Bacteroidetes. J Biol Chem 285:30261–30273. https://doi.org/10.1074/jbc.M110.141788.
7. Moreira LRS, Filho EXF. 2016. Insights into the mechanism of enzymatic hydrolysis of xylan. Appl Microbiol Biotechnol 100:5205–5214. https://doi.org/10.1007/s00253-016-7555-z.
8. Biely P, Singh S, Puchart V. 2016. Towards enzymatic breakdown of complex plant xylan structures: state of the art. Biotechnol Adv 34:1260–1274. https://doi.org/10.1016/j.biotechadv.2016.09.001.
9. Ndeh D, Gilbert HJ. 2018. Biochemistry of complex glycan depolymerisation by the human gut microbiota. FEMS Microbiol Rev 42:146–164. https://doi.org/10.1093/femsre/fuy002.
10. Zhang B, Zhong Y, Dong D, Zheng Z, Hu J. 2022. Gut microbial utilization of xylan and its implication in gut homeostasis and metabolic response. Carbohydr Polym 286:119271. https://doi.org/10.1016/j.carbpol.2022.119271.
11. Briggs JA, Grondin JM, Brumer H. 2021. Communal living: glycan utilization by the human gut microbiota. Environ Microbiol 23:15–35. https://doi.org/10.1111/1462-2920.15317.
12. Watanabe Y, Saito Y, Hara T, Tsukuda N, Aiyama-Suzuki Y, Tanigawa-Yahagi K, Kurakawa T, Moriyama-Ohara K, Matsumoto S, Matsuki T. 2021. Xylan utilisation promotes adaptation of *Bifidobacterium pseudocatenulatum* to the human gastrointestinal tract. ISME Commun 1:62. https://doi.org/10.1038/s43705-021-00066-4.
13. Dodd D, Mackie RI, Cann IKO. 2011. Xylan degradation, a metabolic property shared by rumen and human colonic Bacteroidetes. Mol Microbiol 79:292–304. https://doi.org/10.1111/j.1365-2958.2010.07473.x.
14. Zeybek N, Rastall RA, Buyukkileci AO. 2020. Utilization of xylan-type polysaccharides in co-culture fermentations of *Bifidobacterium* and *Bacteroides* species. Carbohydr Polym 236:116076. https://doi.org/10.1016/j.carbpol.2020.116076.
15. Finegold SM, Li Z, Summanen PH, Downes J, Thames G, Corbett K, Dowd S, Krak M, Heber D. 2014. Xylooligosaccharide increases bifidobacteria but not lactobacilli in human gut microbiota. Food Funct 5:403–614.
16. Li Z, Summanen PH, Komoriya T, Finegold SM. 2015. In vitro study of the prebiotic xylooligosaccharide (XOS) on the growth of *Bifidobacterium* spp and *Lactobacillus* spp. Int J Food Sci Nutr 66:919–922. https://doi.org/10.3109/09637486.2015.1064869.
17. Mäkeläinen H, Saarinen M, Stowell J, Rautonen N, Ouwehand AC. 2010. Xylo-oligosaccharides and lactitol promote the growth of *Bifidobacterium lactis* and *Lactobacillus* species in pure cultures. Benef Microbes 1:139–148. https://doi.org/10.3920/BM2009.0029.
18. Kelly SM, Munoz-Munoz J, van Sinderen D. 2021. Plant glycan metabolism by bifidobacteria. Front Microbiol 12:609418. https://doi.org/10.3389/fmicb.2021.609418.
19. Derrien M, Turroni F, Ventura M, van Sinderen D. 2022. Insights into endogenous *Bifidobacterium* species in the human gut microbiota during adulthood. Trends Microbiol 30:940–947. https://doi.org/10.1016/j.tim.2022.04.004.
20. Shani G, Hoeflinger JL, Heiss BE, Masarweh CF, Larke JA, Jensen NM, Wickramasinghe S, Davis JC, Goonatilleke E, El-Hawiet A, Nguyen L, Klassen JS, Slupsky CM, Lebrilla CB, Mills DA. 2022. Fucosylated human milk oligosaccharide foraging within the species *Bifidobacterium pseudocatenulatum* is driven by glycosyl hydrolase content and specificity. Appl Environ Microbiol 88:e01707-21. https://doi.org/10.1128/AEM.01707-21.
21. Chung The H, Nguyen Ngoc Minh C, Tran Thi Hong C, Nguyen Thi Nguyen T, Pike LJ, Zellmer C, Pham Duc T, Tran T-A, Ha Thanh T, Van MP, Thwaites GE, Rabaa MA, Hall LJ, Baker S. 2021. Exploring the genomic diversity and antimicrobial susceptibility of *Bifidobacterium pseudocatenulatum* in a Vietnamese population. Microbiol Spectr 9:e00526-21. https://doi.org/10.1128/Spectrum.00526-21.
22. Lugli GA, Milani C, Turroni F, Duranti S, Ferrario C, Viappiani A, Mancabelli L, Mangifesta M, Taminiau B, Delcenserie V, van Sinderen D, Ventura M. 2014. Investigation of the evolutionary development of the genus *Bifidobacterium* by comparative genomics. Appl Environ Microbiol 80:6383–6394. https://doi.org/10.1128/AEM.02004-14.
23. Cano PG, Santacruz A, Trejo FM, Sanz Y. 2013. *Bifidobacterium* CECT 7765 improves metabolic and immunological alterations associated with obesity in high-fat diet-fed mice. Obesity (Silver Spring) 21:2310–2321. https://doi.org/10.1002/oby.20330.
24. Sanchis-Chordà J, Del Pulgar EM, Carrasco-Luna J, Benítez-Páez A, Sanz Y, Codoñer-Franch P. 2019. *Bifidobacterium pseudocatenulatum* CECT 7765 supplementation improves inflammatory status in insulin-resistant obese children. Eur J Nutr 58:2789–2800. https://doi.org/10.1007/s00394-018-1828-5.
25. Chen Y, Yang B, Stanton C, Ross RP, Zhao J, Zhang H, Chen W. 2021. *Bifidobacterium pseudocatenulatum* ameliorates DSS-induced colitis by maintaining intestinal mechanical barrier, blocking proinflammatory cytokines, inhibiting TLR4/NF- κB signaling, and altering gut microbiota. J Agric Food Chem 69:1496–1512. https://doi.org/10.1021/acs.jafc.0c06329.
26. Kok CR, Quintero DFG, Niyirora C, Rose D, Li A, Hutkins R. 2019. An in vitro enrichment strategy for formulating synergistic synbiotics. Appl Environ Microbiol 85:e01073-19. https://doi.org/10.1128/AEM.01073-19.
27. Saito Y, Shigehisa A, Watanabe Y, Tsukuda N, Moriyama-Ohara K, Hara T, Matsumoto S, Tsuji H, Matsuki T. 2020. Multiple transporters and glycoside hydrolases are involved in arabinoxylan-derived oligosaccharide utilization in *Bifidobacterium pseudocatenulatum*. Appl Environ Microbiol 86:e01782-20. https://doi.org/10.1128/AEM.01782-20.
28. Liu X, Liu Y, Jiang Z, Liu H, Yang S, Yan Q. 2018. Biochemical characterization of a novel xylanase from *Paenibacillus barengoltzii* and its application in xylooligosaccharides production from corncobs. Food Chem 264:310–318. https://doi.org/10.1016/j.foodchem.2018.05.023.
29. Falck P, Precha-Atsawanan S, Grey C, Immerzeel P, Stålbrand H, Adlercreutz P, Karlsson EN. 2013. Xylooligosaccharides from hardwood and cereal xylans produced by a thermostable xylanase as carbon sources for *Lactobacillus brevis* and *Bifidobacterium adolescentis*. J Agric Food Chem 61:7333–7340. https://doi.org/10.1021/jf401249g.
30. Boonchuay P, Takenaka S, Kuntiya A, Techapun C, Leksawasdi N, Seesuriyachan P, Chaiyaso T. 2016. Purification, characterization, and molecular cloning of the xylanase from *Streptomyces thermovulgaris* TISTR1948 and its application to xylooligosaccharide production. J Mol Catal B Enzym 129:61–68. https://doi.org/10.1016/j.molcatb.2016.03.014.
31. Groussin M, Poyet M, Sistiaga A, Kearney SM, Moniz K, Noel M, Hooker J, Gibbons SM, Segurel L, Froment A, Mohamed RS, Fezeu A, Juimo VA, Lafosse S, Tabe FE, Girard C, Iqaluk D, Nguyen LTT, Shapiro BJ, Lehtimäki J, Ruokolainen L, Kettunen PP, Vatanen T, Sigwazi S, Mabulla A, Domínguez-Rodrigo M, Nartey YA, Agyei-Nkansah A, Duah A, Awuku YA, Valles KA, Asibey SO, Afihene MY, Roberts LR, Plymoth A, Onyekwere CA, Summons RE, Xavier RJ, Alm EJ. 2021. Elevated rates of horizontal gene transfer in the industrialized human microbiome. Cell 184:2053–2067.e18. https://doi.org/10.1016/j.cell.2021.02.052.
32. Amaretti A, Tamburini E, Bernardi T, Pompei A, Zanoni S, Vaccari G, Matteuzzi D, Rossi M. 2006. Substrate preference of *Bifidobacterium adolescentis* MB 239: compared growth on single and mixed carbohydrates. Appl Microbiol Biotechnol 73:654–662. https://doi.org/10.1007/s00253-006-0500-9.
33. Ward RE, Niñonuevo M, Mills DA, Lebrilla CB, German JB. 2006. In vitro fermentation of breast milk oligosaccharides by *Bifidobacterium infantis* and *Lactobacillus gasseri*. Appl Environ Microbiol 72:4497–4499. https://doi.org/10.1128/AEM.02515-05.
34. Pokusaeva K, Fitzgerald GF, Van Sinderen D. 2011. Carbohydrate metabolism in bifidobacteria. Genes Nutr 6:285–306. https://doi.org/10.1007/s12263-010-0206-6.

35. O'Callaghan A, van Sinderen D. 2016. Bifidobacteria and their role as members of the human gut microbiota. Front Microbiol 7:925.
36. Rodriguez CI, Martiny JBH. 2020. Evolutionary relationships among bifidobacteria and their hosts and environments. BMC Genomics 21:26. https://doi.org/10.1186/s12864-019-6435-1.
37. Liu S, Fang Z, Wang H, Zhai Q, Hang F, Zhao J, Zhang H, Lu W, Chen W. 2021. Gene–phenotype associations involving human-residential bifidobacteria (HRB) reveal significant species- and strain-specificity in carbohydrate catabolism. Microorganisms 9:883. https://doi.org/10.3390/microorganisms9050883.
38. Lin G, Liu Q, Wang L, Li H, Zhao J, Zhang H, Wang G, Chen W. 2022. The comparative analysis of genomic diversity and genes involved in carbohydrate metabolism of eighty-eight *Bifidobacterium pseudocatenulatum* isolates from different niches of China. Nutrients 14:2347. https://doi.org/10.3390/nu14112347.
39. Kato K, Odamaki T, Mitsuyama E, Sugahara H, Xiao J-Z, Osawa R. 2017. Age-related changes in the composition of gut *Bifidobacterium* species. Curr Microbiol 74:987–995. https://doi.org/10.1007/s00284-017-1272-4.
40. Kale MS, Yadav MP, Chau HK, Hotchkiss AT, Jr. 2018. Molecular and functional properties of a xylanase hydrolysate of corn bran arabinoxylan. Carbohydr Polym 181:19–123.
41. Ward NE. 2021. Debranching enzymes in corn/soybean meal–based poultry feeds: a review. Poult Sci 100:765–775. https://doi.org/10.1016/j.psj.2020.10.074.
42. Rakoff-Nahoum S, Foster KR, Comstock LE. 2016. The evolution of cooperation within the gut microbiota. Nature 533:255–259. https://doi.org/10.1038/nature17626.
43. Turroni F, Milani C, Duranti S, Mahony J, van Sinderen D, Ventura M. 2018. Glycan utilization and cross-feeding activities by bifidobacteria. Trends Microbiol 26:339–350. https://doi.org/10.1016/j.tim.2017.10.001.
44. Junick J, Blaut M. 2012. Quantification of human fecal *Bifidobacterium* species by use of quantitative real-time PCR analysis targeting the groEL gene. Appl Environ Microbiol 78:2613–2622. https://doi.org/10.1128/AEM.07749-11.
45. Benson AK, David JRD, Gilbreth SE, Smith G, Nietfeldt J, Legge R, Kim J, Sinha R, Duncan CE, Ma J, Singh I. 2014. Microbial successions are associated with changes in chemical profiles of a model refrigerated fresh pork sausage during an 80-day shelf life study. Appl Environ Microbiol 80:5178–5194. https://doi.org/10.1128/AEM.00774-14.
46. Andrews S. 2010. FastQC: a quality control tool for high throughput sequence data.
47. Del Fabbro C, Scalabrin S, Morgante M, Giorgi FM. 2013. An extensive evaluation of read trimming effects on Illumina NGS data analysis. PLoS One 8:e85024. https://doi.org/10.1371/journal.pone.0085024.
48. Bankevich A, Nurk S, Antipov D, Gurevich AA, Dvorkin M, Kulikov AS, Lesin VM, Nikolenko SI, Pham S, Prjibelski AD, Pyshkin AV, Sirotkin AV, Vyahhi N, Tesler G, Alekseyev MA, Pevzner PA. 2012. SPAdes: a new genome assembly algorithm and its applications to single-cell sequencing. J Comput Biol 19:455–477. https://doi.org/10.1089/cmb.2012.0021.
49. Darling ACE, Mau B, Blattner FR, Perna NT. 2004. Mauve: multiple alignment of conserved genomic sequence with rearrangements. Genome Res 14:1394–1403. https://doi.org/10.1101/gr.2289704.
50. Seemann T. 2014. Prokka: rapid prokaryotic genome annotation. Bioinformatics 30:2068–2069. https://doi.org/10.1093/bioinformatics/btu153.
51. Zhang H, Yohe T, Huang L, Entwistle S, Wu P, Yang Z, Busk PK, Xu Y, Yin Y. 2018. dbCAN2: a meta server for automated carbohydrate-active enzyme annotation. Nucleic Acids Res 46:W95–W101. https://doi.org/10.1093/nar/gky418.
52. Li W, O'Neill KR, Haft DH, DiCuccio M, Chetvernin V, Badretdin A, Coulouris G, Chitsaz F, Derbyshire MK, Durkin AS, Gonzales NR, Gwadz M, Lanczycki CJ, Song JS, Thanki N, Wang J, Yamashita RA, Yang M, Zheng C, Marchler-Bauer A, Thibaud-Nissen F. 2021. RefSeq: expanding the Prokaryotic Genome Annotation Pipeline reach with protein family model curation. Nucleic Acids Res 49:D1020–D1028. https://doi.org/10.1093/nar/gkaa1105.
53. Delmont TO, Eren AM. 2018. Linking pangenomes and metagenomes: the *Prochlorococcus* metapangenome. PeerJ 6:e4320. https://doi.org/10.7717/peerj.4320.
54. Eren AM, Esen ÖC, Quince C, Vineis JH, Morrison HG, Sogin ML, Delmont TO. 2015. Anvi'o: an advanced analysis and visualization platform for 'omics data. PeerJ 3:e1319. https://doi.org/10.7717/peerj.1319.
55. Wheeler TJ, Eddy SR. 2013. nhmmer: DNA homology search with profile HMMs. Bioinformatics 29:2487–2489. https://doi.org/10.1093/bioinformatics/btt403.
56. Buchfink B, Reuter K, Drost H-G. 2021. Sensitive protein alignments at tree-of-life scale using DIAMOND. Nat Methods 18:366–368. https://doi.org/10.1038/s41592-021-01101-x.
57. Busk PK, Pilgaard B, Lezyk MJ, Meyer AS, Lange L. 2017. Homology to peptide pattern for annotation of carbohydrate-active enzymes and prediction of function. BMC Bioinformatics 18:214. https://doi.org/10.1186/s12859-017-1625-9.
58. Yang J, Rose DJ. 2014. Long-term dietary pattern of fecal donor correlates with butyrate production and markers of protein fermentation during in vitro fecal fermentation. Nutr Res 34:749–759. https://doi.org/10.1016/j.nutres.2014.08.006.
59. Christen M, Thomsen F, Hasman H, Westh H, Lya Kaya H, Lund O. 2017. RUCS: rapid identification of PCR primers for unique core sequences. Bioinformatics 33:3917–3921. https://doi.org/10.1093/bioinformatics/btx526.
60. Caporaso JG, Kuczynski J, Stombaugh J, Bittinger K, Bushman FD, Costello EK, Fierer N, Gonzalez Peña A, Goodrich JK, Gordon JI, Huttley GA, Kelley ST, Knights D, Koenig JE, Ley RE, Lozupone CA, McDonald D, Muegge BD, Pirrung M, Reeder J, Sevinsky JR, Turnbaugh PJ, Walters WA, Widmann J, Yatsunenko T, Zaneveld J, Knight R. 2010. QIIME allows analysis of high-throughput community sequencing data. Nat Methods 7:335–336. https://doi.org/10.1038/nmeth.f.303.
61. Callahan BJ, McMurdie PJ, Rosen MJ, Han AW, Johnson AJA, Holmes SP. 2016. DADA2: high-resolution sample inference from illumina amplicon data. Nat Methods 13:581–583. https://doi.org/10.1038/nmeth.3869.
62. Bolyen E, Rideout JR, Dillon MR, Bokulich NA, Abnet CC, Al-Ghalith GA, Alexander H, Alm EJ, Arumugam M, Asnicar F, Bai Y, Bisanz JE, Bittinger K, Brejnrod A, Brislawn CJ, Brown CT, Callahan BJ, Caraballo-Rodríguez AM, Chase J, Cope EK, Da Silva R, Diener C, Dorrestein PC, Douglas GM, Durall DM, Duvallet C, Edwardson CF, Ernst M, Estaki M, Fouquier J, Gauglitz JM, Gibbons SM, Gibson DL, Gonzalez A, Gorlick K, Guo J, Hillmann B, Holmes S, Holste H, Huttenhower C, Huttley GA, Janssen S, Jarmusch AK, Jiang L, Kaehler BD, Bin Kang K, Keefe CR, Keim P, Kelley ST, Knights D, et al. 2019. Reproducible, interactive, scalable and extensible microbiome data science using QIIME 2. Nat Biotechnol 37:852–857. https://doi.org/10.1038/s41587-019-0209-9.
63. Quast C, Pruesse E, Yilmaz P, Gerken J, Schweer T, Yarza P, Peplies J, Glöckner FO. 2013. The SILVA ribosomal RNA gene database project: improved data processing and web-based tools. Nucleic Acids Res 41:D590–D596. https://doi.org/10.1093/nar/gks1219.